Limnol. Oceanogr., 49(2), 2004, 555–565

Sources and cycling of carbonyl sulfide in the Sargasso Sea

Gregory A. Cutter, Lynda S. Cutter, and Katherine C. Filippino[1]
Department of Ocean, Earth, and Atmospheric Sciences, Old Dominion University, Norfolk, Virginia 23529-0276

Abstract

The cycling of the radiatively important gas carbonyl sulfide (OCS) was studied in surface waters of the Sargasso Sea. In August 1999, surface OCS concentrations averaged 8.6 pmol L^{-1}, showed minor diel variations, and varied little with depth. An OCS precursor, total dissolved organic sulfur (DOS), was lowest at the surface (40 nmol L^{-1}) and increased with depth. The photoproduction rate of OCS from in situ incubations averaged 9.6 pmol L^{-1} h^{-1}, whereas dark production was 7.0 pmol L^{-1} h^{-1}. Apparent quantum yields were 10^{-5}–10^{-7} from 313–436 nm and varied with the water depth irradiated. In March 2000, there were strong diel variations in surface OCS (highest in late afternoon; overall average, 16.9 pmol L^{-1}). Depth profiles in the afternoon showed surface water maxima and decreases with depth, whereas DOS had a surface maximum of 419 nmol L^{-1} and decreased with depth. Dark production was 4.0 pmol L^{-1} h^{-1}. Modeling of the diel cycle suggested a photoproduction rate of 16.4 pmol L^{-1} h^{-1}. Overall, the photochemical production of OCS strongly depended on DOS and chromophoric dissolved organic matter, whereas dark production was influenced by the presence of particles and perhaps microbial respiration, showing a direct biotic influence on OCS cycling.

Of the sulfur gases emitted from the ocean (dimethyl sulfide, carbonyl sulfide [OCS], and hydrogen sulfide; Andreae 1990), perhaps the most attention has been paid to dimethyl sulfide because of its potential marine biogeochemistry-climate feedbacks (Charlson et al. 1987). However, the oceanic source of OCS is also quantitatively significant, because this gas has an extremely long tropospheric residence time (1–4 yr; Khalil and Rasmussen 1984) and diffuses into the stratosphere, where it maintains the stratospheric sulfate aerosol layer and thereby affects the planetary radiation budget (Crutzen 1976; Turco et al. 1980; Hofmann 1990). Moreover, the hydrolysis of OCS produces dissolved hydrogen sulfide, which can then affect the cycling of many trace metals (Cutter et al. 1999). Thus, the marine cycling of OCS has both atmospheric and oceanic consequences.

Unlike the other marine sulfur gases, OCS has extreme temporal and spatial variations in the ocean. The diel changes in surface OCS first reported by Ferek and Andreae (1984) led those workers to suggest a photochemical production mechanism. Additions of dissolved organic sulfur compounds such as dimethylsulfoniopropionate (DMSP), dimethyl sulfoxide, dimethyl sulfide, methionine, cysteine, and glutathione show that the organic sulfides, particularly glutathione, have the greatest yields of OCS during irradiation (Ferek and Andreae 1984; Zepp and Andreae 1994; Flöck et al. 1997). Studies of the wavelength dependence of OCS photoproduction (apparent quantum yields) in coastal (Zepp and Andreae 1994) and open ocean waters (Weiss et al. 1995*a*) have shown that OCS formation is primarily in the ultraviolet (UV) spectrum, and that the reaction is actually photosensitized by chromophoric dissolved organic matter (CDOM) rather than being a direct photochemical oxidation of dissolved organic sulfur (DOS) compounds. The photosensitized reaction can explain the 100× OCS concentration difference between coastal and open ocean waters (Uher and Andreae 1997). The results of more recent laboratory studies (Pos et al. 1998) have demonstrated that the OCS reaction may involve the production of several sulfide radicals that then react with carbonyl compounds to yield OCS. Of interest, Pos et al. (1998) suggested that this sulfur radical pathway could also produce OCS in the dark. The nonphotochemical, or dark, source of OCS is receiving increasing attention because it can maintain higher OCS concentrations (and saturation) and therefore affect the global OCS budget (Flöck and Andreae 1996; Preiswerk and Najjar 2000; von Hobe et al. 2001). Depth profiles of OCS (Radford-Knoery and Cutter 1994) have always shown the presence of OCS well below the photic zone, necessitating a ''dark'' source when one considers the loss by hydrolysis (see below). In anoxic sediments, Zhang et al. (1998) found that the production of OCS is coupled with microbial sulfate reduction and that this is a significant (dark) source of OCS in estuarine and coastal waters. In the Sargasso Sea, Radford-Knoery and Cutter (1994) speculated that OCS in the major thermocline is produced from particulate organic sulfur by oxic microbial respiration. In this respect, the microbial decomposition of cysteine results in the production of carbonyl compounds, including OCS (Cooper 1983), so a biotic source of OCS is not purely speculative. However, incubations of seawater filtered through GF/F glass-fiber filters to exclude particles and larger microbes have also shown dark production of OCS (Flöck and Andreae 1996; Ulshöfer et al. 1996; Uher and Andreae 1997), which suggests an abiotic degradation of DOS compounds. Clearly, more mechanistic studies of dark OCS production are needed.

The losses of OCS in surface waters include turbulent

[1] Present address: Virginia Institute of Marine Science, P.O. Box 1346, Gloucester Point, Virginia 23062.

Acknowledgments

We thank Ollie Zafiriou for serving as the chief scientist and catalyst for these cruises, Alison Featherstone for OCS determinations on the August cruise, the rest of the Diel investigators, especially Norm Nelson for his CDOM data, and the captain and crew of the R/V *Endeavor* for their able assistance. The manuscript was greatly improved by the comments of two diligent reviewers.

This work was supported by NSF grants OCE 9815190 and 9521628 to G. Cutter.

mixing, sea-air exchange (Najjar et al. 1995), and hydrolysis to carbon dioxide and hydrogen sulfide. The hydrolysis reaction is a function of pH, temperature, and salinity (Elliott et al. 1989; Radford-Knoery and Cutter 1994), which results in OCS having a residence time as little as 6 h in tropical waters (28°C) to 50 h in cold (8°C), high latitudes. All of these various production and consumption processes result in a rather dynamic cycle for OCS in surface waters. However, few studies have examined this cycle from a primarily field approach that used experimental manipulations under in situ conditions of light, temperature, CDOM, DOS, etc. The present article presents data on such an experimental program in the Sargasso Sea that was coupled with parallel studies of carbon monoxide, hydrogen peroxide, and CDOM.

Methods

Study site—Sampling and experimental work were conducted in the vicinity of the U.S. JGOFS Bermuda Atlantic Time-series Study station (BATS; 31°40′N, 64°10′W), which was occupied from 5 to 17 August 1999 and 16 to 29 March 2000 using the RV *Endeavor*. To minimize advective influences on OCS concentrations, the ship was kept in the same water mass by following a Lagrangian drifter in August. After the drifter was destroyed in rough seas during the March cruise, a constant geographic position (Eulerian) was held. Correspondingly, the August water column was highly stratified with a 10–25 m mixed layer, whereas, in March, the mixed layer was ~85 m.

Sampling and analyses—Water-column samples were acquired using a peristaltic pumping system (Zhang et al. 1998) for continuous sampling of surface waters and 5-liter Go-Flo bottles deployed on a conductivity-temperature-depth rosette for depth profiles. Both systems were carefully evaluated for OCS contamination (Radford-Knoery and Cutter 1993; Zhang et al. 1998). The pumping system used black five-eighths-inch Bevaline tubing with polyethylene lining that was deployed on a surface following sampler arm (Donoghue et al. 2001) at 1 m or from a PVC vane that directed the tubing upstream at 1–4 m depth, depending on ship roll. Water was peristaltically pumped using silicone tubing at 2 L min^{-1} into a portable laboratory van that housed the analytical systems. The 5-liter Go-Flo bottles were pressurized with 8 psi nitrogen, and the water was transferred into 4-liter collapsible polyethylene cubitainers with no air headspace (Radford-Knoery and Cutter 1993). Once filled, these cubitainers were kept in a 4°C refrigerator until analysis (1.5 h maximum), and samples were hermetically transferred to the analytical system. Water samples for DOS were placed in 40-ml borosilicate glass vials with Teflon-lined caps and placed in an aluminum block in a −20°C freezer, to quick freeze them for storage.

OCS was determined using the procedure of Radford-Knoery and Cutter (1993), in which a 300-ml gas-stripping vessel is filled from a cubitainer or directly from the pump outflow, and OCS is stripped from solution using He, cryogenically trapped, and then determined with gas chromatography–optimized flame photometric detection. The system was calibrated with a OCS permeation device; the detection limit for OCS was 1 pmol L^{-1}, and precision was >10% (relative standard deviation) at 20 pmol L^{-1}. Pumped samples were analyzed in duplicate, with triplicate analyses for depth profile samples.

DOS was determined using a newly developed method (K.C.F. et al. unpubl. data) that involves the selective removal of sulfate followed by the determination of total dissolved sulfur. Sulfate is removed by pumping 8 ml (at 2 ml min^{-1}) of sample through a 0.5-ml cartridge that contains Ba immobilized on a cation exchange resin ($BaSO_4$ precipitation), a 2.5-ml Ag/cation exchange resin cartridge (which removes Cl^- as AgCl), and finally through a strong anion–exchange resin (BioRad AG 4 × 4 in a 0.5-ml cartridge) that removes most of the remaining sulfate; the first 4 ml are discarded, and the final 4 ml are collected in a borosilicate vial. The residual sulfate, typically 50–80 nmol L^{-1}, is determined with ion chromatography. The recovery of DOS through this sulfate removal system was investigated by amending deionized water and 0.2 μm filtered Sargasso Sea water to 1 μmol S L^{-1} with the following: DMSP, glutathione, taurine, Aldrich humic acid (2.75% S), and humic acid isolated from a Virginia coastal salt marsh (3.74% S). These model compounds represent many of the possible types of organic sulfur species that can be found in seawater, ranging from simple organic sulfides to organic sulfates to complex organic sulfur. Recoveries for all compounds except glutathione were >95%, with glutathione having 73% recovery. We are still investigating this low glutathione recovery to see whether some procedural modification can improve it. Total dissolved sulfur was determined using a reductive pyrolysis apparatus that quantitatively reduces all dissolved sulfur compounds to hydrogen sulfide and consists of (1) a quartz tube filled with quartz beads and 6 cm of 20% Pt on alumina in the center, heated to 1,050°C, fitted with a injection port (Teflon-backed silicone septum; water cooled), and purged with ultra–high purity hydrogen; (2) a borosilicate U-tube held at −50°C to remove water vapor; and (3) the OCS/H_2S trapping and detection system described in Radford-Knoery and Cutter (1993) for the determination of H_2S. The sample (10–60 μl) was injected into the furnace using a digital syringe, and the generated H_2S was trapped for 4 min, to achieve full recovery. The amount of H_2S versus volume injected was fitted to a linear curve, with the slope yielding the sample concentration. This method removes the need to correct for blanks caused by the apparatus (i.e., the furnace and catalyst), a frequent problem with DOC determinations (Benner and Strom 1993). Quantitative (100%) recoveries were found for all model compounds tested—sulfate, cysteine, methionine, glutathione, DMSP, taurine, and humic acids. After the level of total dissolved sulfur was determined, DOS was then the difference between the total and the residual sulfate. The precision for DOS was >10% (relative standard deviation) at 100 nmol S L^{-1}, and the detection limit was 15 nmol S L^{-1}.

In situ incubations—To measure in situ photochemical production of OCS, an ''optical buoy'' (Taylor et al. pers. comm.) system was used. Quartz sample flasks were held upside down in wire cages that were suspended at different

depths on a weighted polyester line that was attached to the center of the buoy (an aluminum pipe tetrahedron with floats), to minimize shading. Water for the buoy samples was obtained from 8–100 m (depth varied with deployment; see ''Results'' section) using a 30-liter Go Flo bottle. On recovery, it was pressurized with N_2, and water was transferred with minimal air entrainment (i.e., using procedures similar to those for an oxygen sample) into a 50-liter glass carboy that was then sparged with OCS-free air for 4 h. Under low light, this water was transferred by siphon into the 500-ml quartz round-bottom flasks (without head space) and placed in cages. Dark controls consisted of identical flasks covered with aluminum foil. Controls were deployed at two buoy depths, and additional controls were kept in the dark under running seawater (i.e., surface water temperature). Each cage was kept covered until just before the buoy was deployed at dawn. The buoy was then released and recovered ~6 h later. As the flasks were recovered, they were immediately covered and placed in a 4°C refrigerator to minimize hydrolysis. OCS was determined at time 0 and at each depth interval using the methods described above.

Dark incubations—Water for dark incubations in August 1999 was obtained using the 30-liter Go Flo bottle, passed through an all Teflon digital flowmeter/accumulator (to measure the water volume), and put directly into 3-liter Tefzel gas sampling bags. These bags had the septa fitting replaced with a two-way valve and one-eighth-inch Teflon tubing that allowed overlying air to be completely removed and sample withdrawal. Water for the dark incubations was either 0.4 μm filtered (control), unfiltered unfiltered, and amended with particles (a 142 mm, 0.4 μm polycarbonate filter through which 30 liters of seawater (90 and 8 m depths) had been passed) or 0.4 μm filtered and containing an unused polycarbonate filter (filter control). The filled gas bags were placed in black plastic bags and incubated in an insulated, covered container through which surface seawater was pumped. Water samples were withdrawn at four time points using a 100-ml glass gas tight syringe and analyzed as described above for OCS.

Quantum yields—For these studies, water was collected using the 30-liter Go Flo bottle during the August 1999 cruise, pressure filtered through a 0.2-μm polycarbonate filter, and placed in solvent-cleaned, amber borosilicate glass bottles that were stored at 4°C for no more than 2 months before use. At the shore-side laboratory, this water was then transferred using a 100-ml gas tight syringe into a 31-cm path length, 117-ml borosilicate glass cell with quartz windows and Teflon stoppers (no headspace was allowed) that was thermostatically held at 20°C (OCS was determined on a second aliquot to determine the $t = 0$ concentration). The cell was placed in an irradiation system described by Andrews et al. (2000) and irradiated for 1.0 h at 313 and 365 nm, 2.0 h for 405 nm, and 6.0 h for 436 nm. OCS was then determined in the irradiated solution. All irradiations and determinations were done in triplicate. Knowing the light flux (from actinometry and a radiometer sensor), the CDOM absorption coefficients, and OCS production rate, the apparent quantum yields were calculated (Andrews et al. 2000).

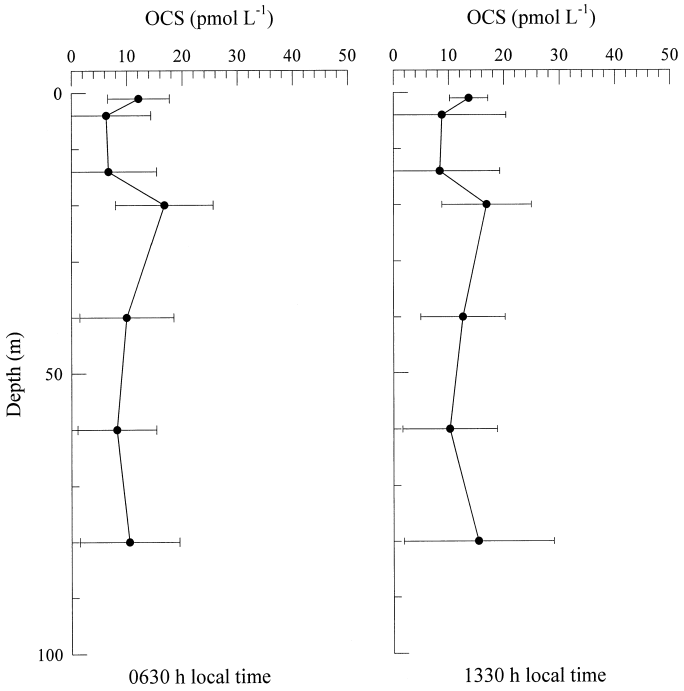

Fig. 1. A composite (mean ± standard deviation) of all depth profiles for OCS taken in the morning ($n = 9$) and afternoon ($n = 10$) from 5 to 17 August 1999 near the BATS station in the Sargasso Sea.

It should also be noted that inner filter, or self-shading, effects (Hu et al. 2002) were negligible (absolute coefficient × path length = 0.005).

Results

August 1999—The timing of the August cruise was selected to examine OCS cycling under maximum stratification and shallow mixed layer, deep UV penetration, and low CDOM from photobleaching. A composite of vertical profiles over 11 d, taken just after sunrise and in the afternoon, to highlight the maximum photochemical production of OCS, is shown in Fig. 1. From the surface to the upper thermocline (the mixed layer averaged 25 m during this period), OCS showed surprisingly little variation with depth, with near-surface (2 m) values averaging 12.1 ± 5.6 pmol L^{-1} ($n = 9$) in the morning and 13.7 ± 3.5 pmol L^{-1} ($n = 11$) in the afternoon. The average concentrations in these profiles in the upper 20 m agree well with those of Von Hobe et al. (2001), which were taken at the same depths during this cruise using an independent sampling and analytical system. A surface time series for OCS was also obtained, but these data are thoroughly discussed in Von Hobe et al. (2001). The profiles of the potential OCS precursor, DOS, for the August 1999 cruise, and for 1 yr earlier at the BATS site (to demonstrate method consistency), are shown in Fig. 2A. In both summer profiles, DOS displayed a surface minimum and an increase into the upper thermocline, although in August 1999 a subsurface maximum was apparent. These are the first oceanic profiles for DOS, so no comparisons with previous work can be made, but the surface minimum

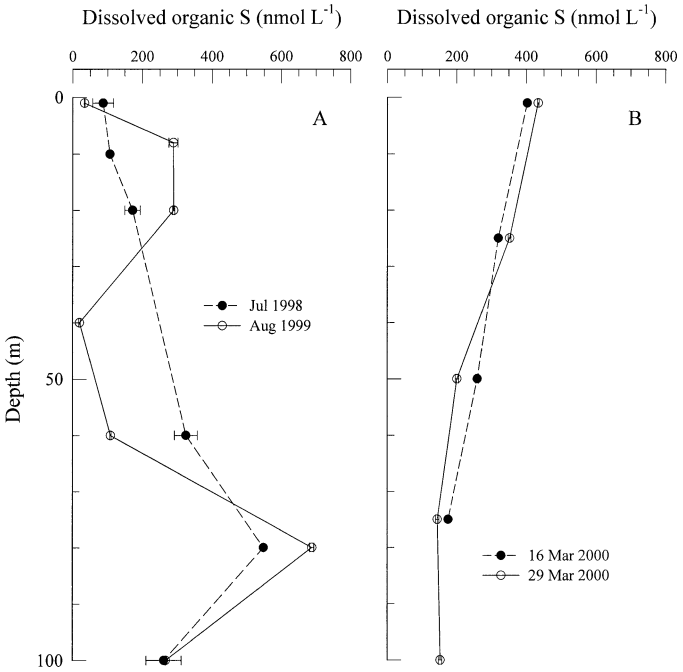

Fig. 2. Depth profiles for DOS taken near the BATS station in the Sargasso Sea in (A) July 1998 and August 1999 and (B) March 2000. Note that, if error bars are not apparent, they are smaller than the symbol.

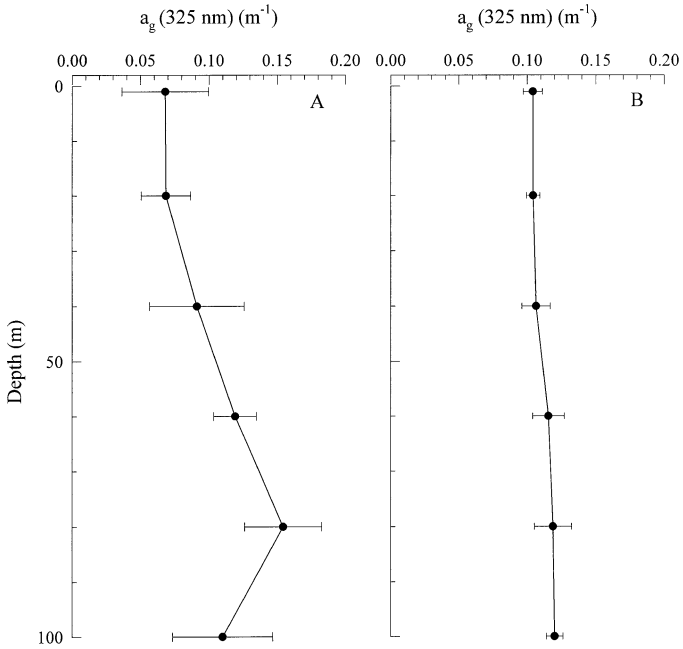

Fig. 3. Average depth profiles (mean ± standard deviation) of CDOM absorption coefficients (a_g, 325 nm) taken near the BATS station in the Sargasso Sea in (A) July–August 1999 and (B) March 2000. Data were provided by N. Nelson.

and increase with depth were present in two different years, and the distributions of DOS were very similar to summertime profiles of the CDOM absorption coefficient in the Sargasso Sea (Nelson et al. 1998; Fig. 3A).

The photochemical production rate of OCS was measured using optical buoys deployed three times at six–seven depths (Fig. 4). CDOM absorption coefficients varied by a factor of 2 with depth during the summer (Fig. 3A), and DOS varied by a factor of 20 (Fig. 2A). Thus, water used to fill the quartz flasks was obtained from two depths in the mixed layer (8 and 24 m) and two depths in the upper thermocline (40 and 100 m), to examine the potential effects of short-term mixing of these and other constituents (i.e., what might occur if these deeper waters were upwelled). Dark production also introduces OCS to the flasks, and dark bottle controls were included with each deployment (dark bottle concentrations are not shown in Fig. 4). Because OCS hydrolysis affects the concentration in the dark (and light) flasks, dark production was calculated using an equation given in Ulshöfer et al. (1996):

$$[\mathrm{OCS}]_t = [\mathrm{OCS}]_0 \times e^{-h \cdot t} + (q/h) \times (1 - e^{-h \cdot t}) \quad (1)$$

where $[\mathrm{OCS}]_t$ is the measured concentration at time t (total deployment time), $[\mathrm{OCS}]_0$ is the $t = 0$ concentration, h is the hydrolysis rate constant (calculated using the measured temperature, pH, and salinity for each deployment, and the equations in Radford-Knoery and Cutter 1994), and q is the zero-order dark production rate. The dark production rates calculated in this fashion averaged 7.4 ± 1.8 pmol L^{-1} h^{-1} ($n = 4$) and are listed in Fig. 4.

In the primary optical buoy results, the most obvious feature in Fig. 4 is that the OCS concentrations in the flasks (left panels for each buoy) were 5–10 times higher than those in the water column (Fig. 1). This can be explained by several factors. Water processing for the deployments introduced contaminant OCS, such that the $t = 0$ values ranged 18–31 pmol L^{-1} (depending on the deployment). Even though the experiments started with elevated concentrations, this was not a significant problem, because we were measuring changes over time (final concentrations were 3–5 times the $t = 0$ values). In addition, losses by sea-air exchange and mixing, the later of which is a significant control on OCS in surface waters (Najjar et al. 1995), were absent in the buoy incubations. This closed system then allowed the concentration of OCS to rise well above ambient levels. To quantify this effect, Eq. (1), which has no mixing or sea-air exchange, can be applied to the deepest OCS flask in buoy 8 (40 m; Fig. 4) to compute an apparent dark production rate because, to a first approximation, photochemical production was negligible; this can then be compared with the actual dark incubation rate for that deployment. In this manner, the calculated dark production at 40 m was 8.1 pmol L^{-1} h^{-1}, which was only 29% higher than the observed dark production rate of 6.3 pmol L^{-1} h^{-1} (Fig. 4). This calculation demonstrates that, in the absence of mixing, the observed flask concentrations easily can be reached; in the upper depths, photoproduction would then elevate OCS concentrations further.

With representative concentrations from the buoys, the next issue was how to calculate OCS photoproduction rates, given the continuous loss by hydrolysis. In this respect, the optical buoy approach has never been applied to the study of OCS. The simplest calculation, light flask minus dark

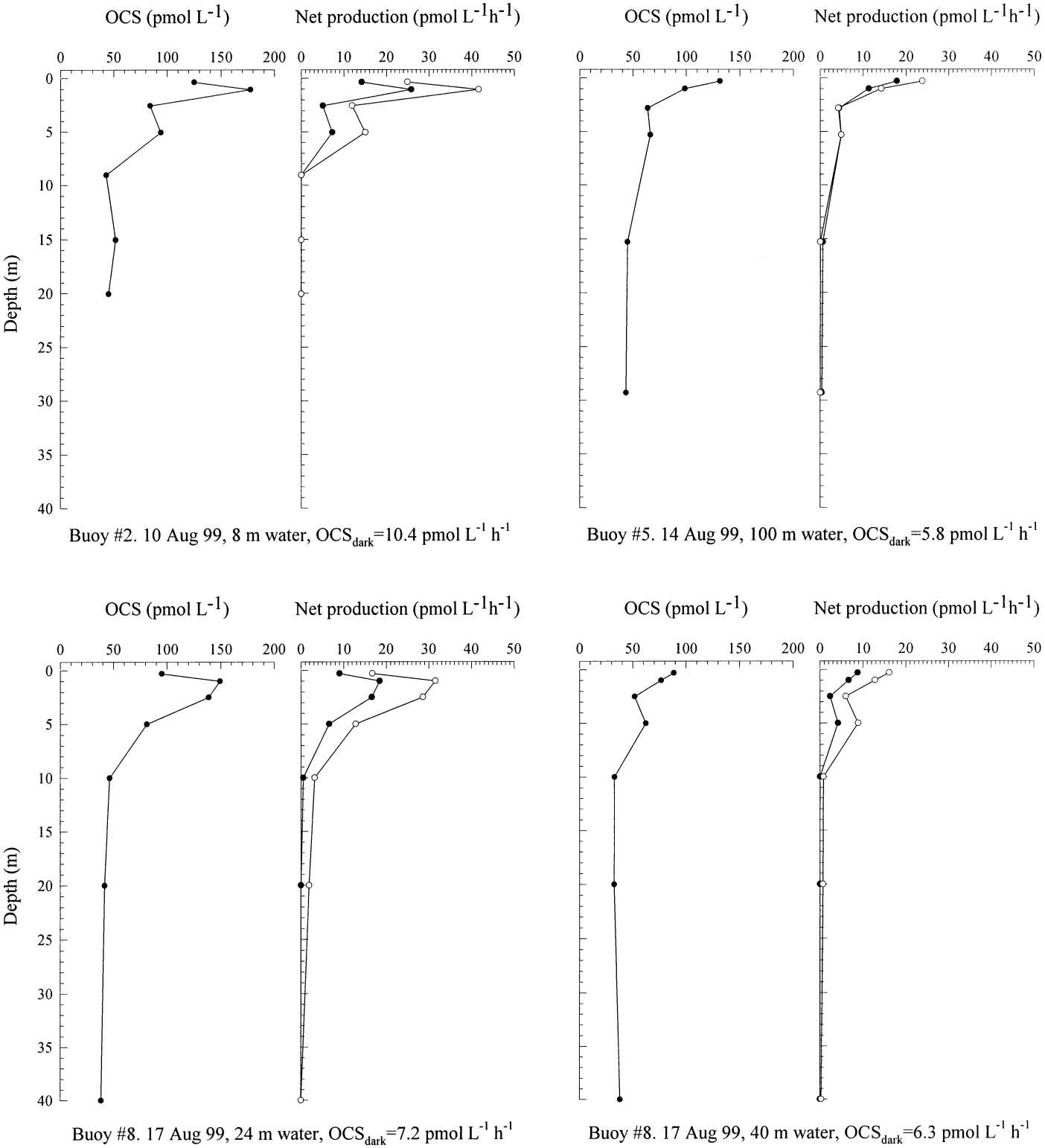

Fig. 4. Optical buoy profiles for the Sargasso Sea. In each set of two per buoy, the left panel shows the average OCS concentration in flasks from each depth. The right panel displays the net production rate computed using a simple difference calculation ($OCS_{light} - OCS_{dark}$/ deployment time; filled circles) and using Eq. 2 in the text (open symbols). The computed dark production rate (OCS_{dark}) for each buoy is also shown.

flask OCS divided by the incubation time, assumed that hydrolysis affects the dark and light flasks equally. Because the OCS concentrations in each differed by no more than a factor of 2 near the surface and were nearly identical at depths >10 m, this may not be an unreasonable assumption; the rates by difference were plotted in the right-hand panels for each buoy in Fig. 4. Because the difference method essentially ignored hydrolysis, these rates in Fig. 4 likely underestimate the true photoproduction rates. Alternatively, the light + dark production equation of Flöck et al. (1997) for irradiation experiments can be used to calculate the light production rates

$$[\mathrm{OCS}]_t = [\mathrm{OCS}]_0 \times e^{-h \cdot t} + [(p \times I + q)/h] \times (1 - e^{-h \cdot t}) \quad (2)$$

This equation has the same variables as Eq. (1) but adds the light production rate constant p and UV irradiation, I; together, $p \times I$ is the light production rate. The primary assumption in this equation is that the light flux is *constant.* This certainly is not true for actual in situ incubations, but, for the short (5–6 h) daytime deployment times used in our experiments, the observed surface irradiance varied by only 10–28%, with an average of 19%. Thus, we assumed that the light was roughly constant, so that Eq. (2) applies; the results are also plotted in Fig. 4. If we only consider buoy 5 (Fig. 4), the agreement between calculations is excellent, but, overall, the constant light rates were twice those of the difference method. The application of Eq. (2) includes hydrolysis, and, even with its assumption of constant light, probably yields more accurate rates. These rates will be used for the remainder of the discussions.

The profiles of photochemical production rates for OCS displayed two trends: (1) maxima near the surface and exponential decreases with depth (Fig. 4, buoy 5) and (2) production rates and depth distributions that varied with the water of origin (compare the net production rate profiles for buoys 5 and 8, using 24-m water; Fig. 4). These are the first OCS data obtained from in situ incubations, so we have little with which to compare them, but, for three deployments and four different water types, the profiles were similar to expectations. In particular, previous studies of OCS photochemical production (Zepp and Andreae 1994; Weiss et al. 1995*a*) have demonstrated that most OCS photoproduction occurs in the UV, so the exponential decreases with depth are consistent with UV attenuation and direct measurements made during the cruise (e.g., the 325 nm irradiance was 10% of surface values by 25 m; Nelson unpubl. data). The subsurface maxima seen in buoys 2 and 8, using 24-m water (Fig. 4), were a bit unexpected, and although they could have been due to occasional shading of the 0.3-m flasks (uppermost depth in all the deployments) by the buoy, buoy 8 had flasks with water from two different depths but only one showed the subsurface maximum (Fig. 4). Thus, there may have been effects due to the water itself and differing CDOM absorption coefficients and DOS concentrations (Figs. 2A, 3A).

In addition to the dark flask incubations as part of the optical buoys, tightly controlled incubation experiments were conducted on board ship to elucidate whether the dark production of OCS is derived from dissolved constituents (e.g., CDOM; Flöck et al. 1997; Pos et al. 1998) or the degradation of particulate organic matter (Radford-Knoery and Cutter 1994). The results of one of these experiments for 90-m water, a depth that coincides with the chlorophyll maximum and a particulate organic carbon (POC) concentration of 62 μg L^{-1}, are shown in Fig. 5. Although there was dark production in 0.4 μm filtered water (largely dissolved matter, although some bacteria, viruses, and colloidal matter would be present), the presence of particles had a dramatic effect on OCS production (Fig. 5); amending the solution with even more particles (on a polycarbonate filter) increased production further. To quantify the rates, the data in Fig. 5 were fitted to Eq. (1) using a nonlinear curve fitting routine. The filtered incubation had a rate of 3.6 ± 2.1 pmol L^{-1} h^{-1}, whereas the unfiltered incubation had a rate of 22.1 ± 2.2 pmol L^{-1} h^{-1}, which clearly demonstrates a particle effect. The addition of more particles (filtered from 30 liters and added to 2 liters of the same, unfiltered water, a ~15× enrichment) increased the rate to 37.5 ± 2.9 pmol L^{-1} h^{-1}. Of interest, an identical dark incubation experiment using water from 8 m (POC of 41 μg L^{-1}) did not show this pronounced particle effect, because the filtered and unfiltered rates were essentially the same (filtered, 21.6 ± 3.7 pmol L^{-1} h^{-1}; unfiltered, 17.1 ± 2.4 pmol L^{-1} h^{-1}).

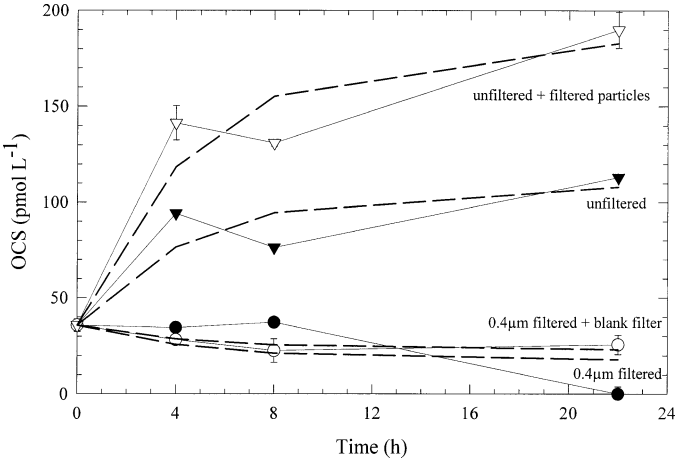

Fig. 5. Results from a 22-h dark OCS production study in August 1999 using water from 90-m depth that was passed through a 0.4-μm filter (filled circles), water that was passed through a 0.4-μm filter and contained an unused 142-mm polycarbonate filter (open circles), unfiltered water (filled triangles), and unfiltered water plus a filter with particles from 30 liters of water from 90-m depth (open triangles). The incubations were carried out at 29.2°C. The dashed lines are the fits of Eq. 1 in the text to each of the treatments' data.

To complement the optical buoy experiments, apparent quantum yields were determined using water from 8 and 40 m, which represented photobleached surface water and subsurface water that could be rapidly mixed to the surface (i.e., potential production after mixing events). The OCS production rate versus wavelength results are shown in Fig. 6A. OCS production normalized to light flux (Joules cm^{-2}), or "action spectra," are shown in Fig. 6B, and the computed apparent quantum yields are given in Table 1. As was expected from the results of previous studies, OCS production was highest at the lower wavelengths but was detectable in the visible (i.e., 436 nm; Fig. 6A,B). The action spectrum

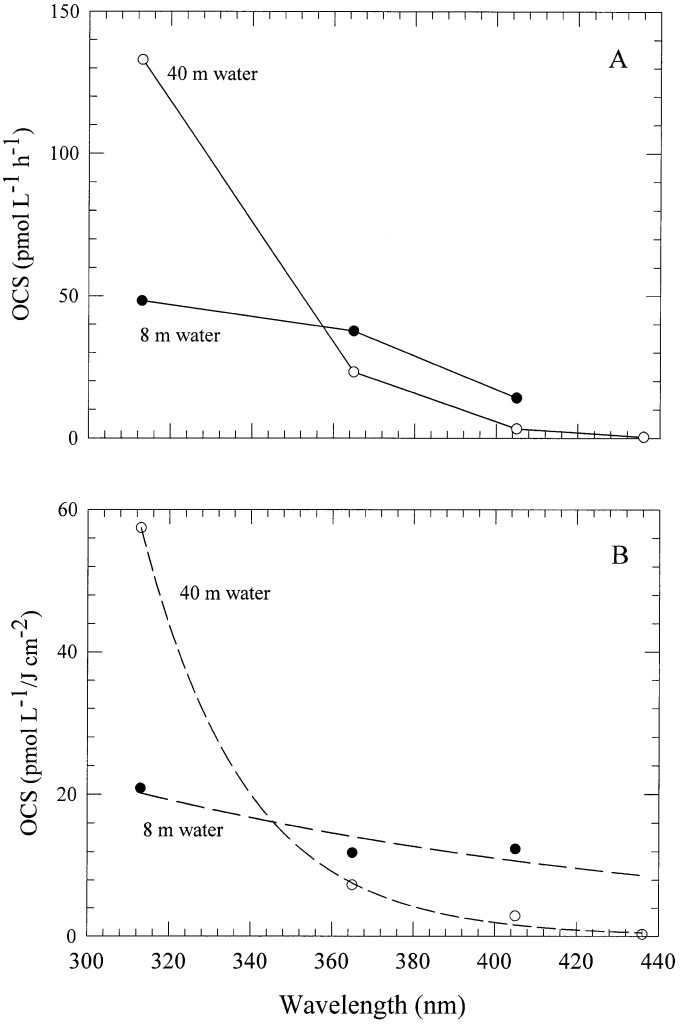

Fig. 6. Results for laboratory irradiations of 8-m (filled circles) and 40-m (open circles) water from the August 1999 cruise, to derive apparent quantum yields for OCS photochemical production. (A) The rate of OCS production of the two water samples as a function of irradiation wavelength. (B) Action spectra for the Sargasso Sea water samples in panel A. The dashed lines are exponential fits to the data [(pmol L^{-1}/J cm^{-2})$_{nm}$ = (pmol L^{-1}/J cm^{-2})$_{313nm}$ × $e^{-B\cdot(313nm)}$], where, for the 8-m sample, B = 0.0069 and r^2 = 0.84, and, for the 40-m sample, B = 0.039 and r^2 = 0.99.

(Fig. 6B) showed the expected exponential decrease with wavelength for 40 m water, but the 8-m spectrum was noticeably flat (poorer exponential fit; note no data for 436 nm). As a result, the 40-m production as a function of the light flux (Fig. 6B) from 313 to 405 nm was 21–48 times that found by Weiss et al. (1995*a*) for Antarctic water, but the 8-m values rose from 13 to 207 times the Weiss et al. values. Similarly, the Sargasso Sea quantum yields were up to two orders of magnitude higher than those of Weiss et al. (Table 1). However, for the two wavelengths that nearly overlap, the agreement with the coastal Gulf of Mexico water used in Zepp and Andreae (1994) was much better (Table 1); this will be discussed below.

March 2000—The focus of the March cruise was essentially the same as August, except there were conditions of

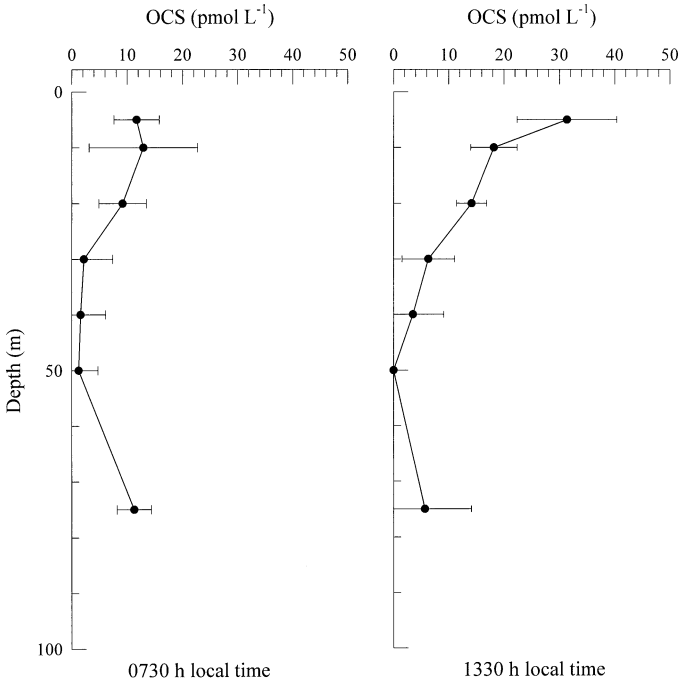

Fig. 7. A composite (mean ± standard deviation) of all depth profiles for OCS taken in the morning (n = 11) and afternoon (n = 9) from 16 to 29 March 2000 near the BATS station in the Sargasso Sea.

greater mixing (deep mixed layer), higher biological productivity, elevated CDOM, and lower temperatures. To remove the problem of correcting optical buoy rates for OCS hydrolysis (as above), 100 nmol L^{-1} zinc acetate was added to the optical buoy water to complex and stabilize hydrogen sulfide (Zhang 1999) produced by the hydrolysis reaction. These soluble complexes could then be determined with OCS (Radford-Knoery and Cutter 1993) to derive the full OCS production rate. Unfortunately, this Zn affected CDOM absorption (e.g., $a_g(325)$ = 0.12^{-1} without zinc and 0.02^{-1} with zinc); as a result, very little OCS was produced in the buoy incubations. Thus, there are no optical buoy data to report. However, the dark flask incubations (no zinc addi-

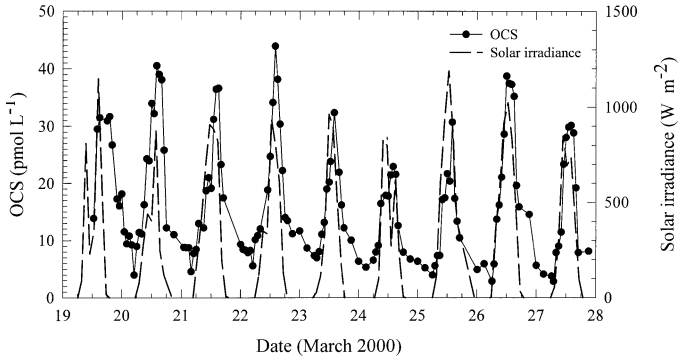

Fig. 8. A time series for OCS at 1–4 m (depending on sea state) and solar irradiance near the BATS station from 19 to 28 March 2000. OCS determinations were made in duplicate, and the average was plotted.

Table 1. Apparent quantum yields for Sargasso Sea water taken in August 1999.

Wavelength (nm)	a_g, 8 m (m^{-1})	a_g, 40 m (m^{-1})	Quantum yields			
			This work		Weiss et al. (1995*a*)	Zepp and Andreae (1994)*
			8 m	40 m		
313	0.203	0.202	$4.0\pm0.8\times10^{-6}$	$1.1\pm0.4\times10^{-5}$	2.5×10^{-7}	$0.4–1.4\times10^{-6}$
365	0.101	0.091	$3.9\pm1.1\times10^{-6}$	$2.7\pm0.2\times10^{-6}$	9.3×10^{-8}	6.4×10^{-7}
405	0.070	0.042	$5.3\pm1.4\times10^{-6}$	$2.0\pm0.3\times10^{-6}$	1.9×10^{-8}	ND
436	0.049	0.028	ND	$2.8\pm0.5\times10^{-7}$	ND	ND

a_g, CDOM absorption coefficient; ND, not determined.
* Actual wavelengths were 310 and 360 nm.

tion) yielded an average dark production rate for 3 m water of 4.0 ± 0.5 pmol L^{-1} h^{-1} (n = 4 deployments) at a temperature of 20.5°C, almost half those in August 1999 (temperature 27.5°C).

The average vertical profile of OCS in March (Fig. 7) was quite similar to the August profile (Fig. 1) in the early morning, with little vertical structure (average surface value of 11.7 ± 4.1 pmol L^{-1}). However, the late afternoon profiles showed a substantial enrichment of OCS at the surface (31.4 ± 9.0 pmol L^{-1}) that was much like those found at this site by other researchers (Radford-Knoery and Cutter 1994), as well as at other ocean stations (Ferek and Andreae 1984; Flöck and Andreae 1996). Like the afternoon OCS profiles, the profiles of DOS in March (Fig. 2B; note that two profiles are shown) were substantially different than those in August (Fig. 2A)—there was an average surface maximum of 419 nmol L^{-1}, which is 12 times greater than the value in August, and a decrease with depth. Thus, the potential precursors of OCS that are contained in DOS were much higher during March than August. Additionally, March CDOM absorption coefficients were nearly twice the August values (Fig. 3B).

The vertical profile results suggest a strong diel cycle, but the actual time series for OCS and solar irradiance in Fig. 8 clearly document how strong this cycle is. Over the 9-day period, surface OCS varied from 3 to 44 pmol L^{-1}, with an average of 16.9 ± 10.2 pmol L^{-1} (n = 143), and lagged the maximum solar irradiance by an average of 1.7 ± 1.0 h (n = 9). The magnitude of this diel change was substantially larger than that in August (33% in August and 60% in March), and the average concentration was a factor of 2 higher. The lag time between OCS and light was slightly shorter than those reported in other waters (2–3 h; Andreae and Ferek 1992; Ulshöfer et al. 1995; Weiss et al. 1995*b*) but was similar to the August timing (Von Hobe et al. 2001). The lowest OCS concentrations were found at sunrise, which averaged 5.2 ± 1.7 pmol L^{-1} (n = 8), which is slightly higher than those in August (Von Hobe et al. 2001).

Discussion

Photochemical production—The production of OCS in the surface ocean clearly has a dominant photochemical route, as has been shown by previous investigators, and should depend on the light flux and concentration of the photosensitizers (i.e., CDOM; Zepp and Andreae 1994; Weiss et al. 1995*a*; Pos et al. 1998) and the concentration—or, more specifically, the exact composition—of the DOS precursors (Zepp and Andreae 1994; Flöck et al. 1997). In a qualitative sense, the doubling of surface OCS concentrations between August 1999 and March 2000 (Figs. 1, 7) occurred in the presence of greater CDOM absorption coefficients (Fig. 3) and DOS concentrations (Fig. 2) and a slower rate of hydrolysis (~50% reduction). A more direct comparison of the effects of DOS and CDOM is available with the optical buoy 8 results (Fig. 4), in which waters from two different depths were incubated simultaneously (same light fluxes at each depth). Because >95% of the OCS production occurred in the upper 10 m (Fig. 4) and to more accurately quantify surface mixed layer production rates, depth-integrated average production rates (pmol L^{-1} h^{-1}) were computed for the upper 10 m of all buoy deployments. For buoy 8, water from 24 m (Fig. 4), with a DOS of ~280 nmol L^{-1} (Fig. 2A), had a depth-integrated average OCS production rate of 15.2 pmol L^{-1} h^{-1}, whereas that for water from 40 m (DOS, 20 nmol L^{-1}) had an average rate of 6.8 pmol L^{-1} h^{-1}; the 40-m CDOM absorption coefficient was 29% higher than that of the 24-m water (Fig. 3A).

Comparisons between the other buoy deployments must be made with caution, because the light fluxes differed. However, the results for buoy 2, using 8-m water (Fig. 4), which had a depth-integrated average production rate of 12.5 pmol L^{-1} h^{-1}, agreed reasonably well with results from the 24-m water data of buoy 8. Both had similar DOS and CDOM (Figs. 2A, 3A). Thus, the concentration of DOS appears to affect the photochemical production rate of OCS. However, the 100-m water optical buoy results (buoy 5 in Fig. 4) yielded a depth-averaged production rate of only 3.8 pmol L^{-1} h^{-1}, in spite of its water having elevated DOS (Fig. 2A) and the highest CDOM absorption coefficient (Fig. 3A). This behavior may be a result of the differing composition of DOS itself (i.e., it is the total of all organic sulfur forms). Overall, the average photoproduction rate for waters from the surface mixed layer (i.e., buoys 2 and 8, 24 m; Fig. 4) was 13.9 pmol L^{-1} h^{-1}, which corresponds to 0.2 nmol L^{-1} d^{-1} (13-h photoperiod). As was noted previously, there are no other optical buoy data in oceanic waters for direct comparison with these data. However, Weiss et al. (1995*a*) used apparent quantum yield and solar irradiance data to estimate surface-water OCS photoproduction at 0.07–0.10 nmol L^{-1} d^{-1} in the Pacific Ocean. In the Mediterranean Sea, Ulshöfer et al. (1996) obtained rates of 0.07 nmol L^{-1} d^{-1} using model fits to a 3-m OCS time series and ~0.09 nmol L^{-1} d^{-1} from

deck-board incubations (i.e., 0 m depth). The Sargasso Sea rate was comparable to these other values, keeping in mind the different approaches for their calculation and, therefore, the depths they represent (i.e., 0–10 m for the Sargasso Sea).

Although the optical buoys provided direct measures of photochemical OCS production, the quantitative relationship between light fluxes and production is best quantified by apparent quantum yields (AQYs). In this respect, the results in Table 1 and Fig. 6 show that the 8- and 40-m waters have very different action spectra and that the Sargasso Sea AQYs are more like those for coastal Gulf of Mexico waters (Zepp and Andreae 1994) than for the open ocean (South Pacific; Weiss et al. 1995*a*). These two samples had different CDOM absorption coefficients (Fig. 3A) and DOS concentrations (Fig. 2A), and the optical buoys clearly showed how these can affect production. In addition, the works of Zepp and Andreae (1994) and Flock et al. (1997) showed that variations in the actual compounds that make up DOS (e.g., glutathione, methionine, and DMSP) affect the production rate, and, hence the AQY, of OCS. Of interest, available AQY data (Zepp and Andreae 1994; Weiss et al. 1995*a*) have shown deviations in the action spectra slope between 320 and 340 nm that were somewhat similar to that of the 8-m sample (Fig. 6B), although the missing 436-nm data do not allow a complete comparison. In terms of the AQYs at both depths from the Sargasso Sea appearing more like those in coastal waters, the Sargasso Sea absorption coefficients (Table 1) were nearly identical to the Weiss et al. (1995*a*) set. Thus, the explanation likely involves the concentrations and composition of DOS, data that are not available for the Pacific Ocean and Gulf of Mexico samples.

The AQY results in Table 1 and in the literature demonstrate that the photochemical production of OCS is far less efficient than that of another trace gas, CO (e.g., 10^{-3}–10^{-5} over the same wavelength range; Valentine and Zepp 1993). It has been argued that the formation of both gases are linked through a common acyl radical intermediate (Pos et al. 1998), but OCS formation also requires thiyl (RS· from DOS) or sulfhydryl (SH· from bisulfide) radicals (Zepp and Andreae 1994; Pos et al. 1998). It is likely the low AQYs are then caused by the formation of these latter species. Although the AQYs are low overall, production still occurs at longer wavelengths, which allows photochemical contributions to be deeper than those expected strictly from the penetration of UV radiation. This is apparent in the last optical buoy deployment (buoy 8 in Fig. 4), where photochemical production was still measurable at 20–40 m.

Dark production—The subject of dark OCS production was recognized as early as 1994 (Radford-Knoery and Cutter 1994) to be a potentially important source. The average rates measured in the Sargasso Sea, 7.4 pmol L^{-1} h^{-1} in August 1999 and 4.0 pmol L^{-1} h^{-1} in March 2000, were slightly higher than those measured by incubation in other regions (1.5–2.3 pmol L^{-1} h^{-1}; Flöck and Andreae 1996; Ulshöfer et al. 1996), although these previous measurements used filtered rather than whole water. Mechanistically, an abiotic pathway involving thiyl radicals (Flöck et al. 1997; Pos et al. 1998) and one involving the microbial degradation of organic matter (respiration; Radford-Knoery and Cutter 1994; Zhang et al. 1998) have been proposed. In this respect, the data in Fig. 5 show that, although OCS is produced from dissolved (<0.4 μm) organic matter (i.e., perhaps by the abiotic pathway), the presence of particles increases the production rate by a factor of 5–6. Extremely low rates of dark OCS production (e.g., 0.1 pmol L^{-1} h^{-1}) in the deep ocean (Flöck and Andreae 1996) can then be explained not only by the low temperatures but also by low concentrations of particulate organic matter. Although no microbial inhibitor experiments were conducted in our incubations and zooplankton grazers were not specifically excluded, a microbial role in dark OCS production seems to be the most reasonable mechanism, given the well-documented bacterial role in sedimentary (dark) OCS production (Zhang et al. 1998). Clearly, more studies are needed on this important facet of OCS cycling.

Comparing the measured rates of dark OCS production in August 1999 (Fig. 4) with the depth-integrated average photoproduction rates from the buoy deployments (0–10 m; given above), dark production averaged 61 $\pm$ 10% ($n = 4$) of the total production over a 24-h period, which is in reasonable agreement with the 39–57% independently calculated by Von Hobe et al. (2001) for the upper 5 m during the same period.

Synthesis—The concentration and temporal behavior of OCS in surface waters are controlled by the balance between photochemical (Figs. 4, 6) and dark (Fig. 5) production and losses by hydrolysis, air-sea exchange, and mixing with deeper, low-OCS waters. The mathematical expression of this balance (modified after von Hobe et al. 1999) is

$$\begin{aligned} d[\mathrm{OCS}]_{\mathrm{surf}}/dt = {} & P_{\mathrm{UV}} \times I_t + Q - k_{hyd} \times [\mathrm{OCS}]_t \\ & - (k_w/z_m) \times ([\mathrm{OCS}]_{\mathrm{surf}} - [\mathrm{OCS}]_{\mathrm{air}}/H) \\ & - (K_z/z_m) \times (d[\mathrm{COS}]_t/dz) \end{aligned} \quad (3)$$

where light production has been simply written as a zero-order production rate constant (derived from quantum yield experiments or optical buoy results) times the UV irradiation at the surface (i.e., no depth dependence for only the surface behavior). Dark production (Q) was assumed to be a constant rate, even though it is affected by particles, dissolved precursors, and temperature (von Hobe et al. 2001). To compute OCS losses, hydrolysis could be accurately calculated using the formulation of Radford-Knoery and Cutter (1994), whereas sea-air exchange was derived from the Liss and Merlivat (1986) approach (k_w adjusted for wind speed and normalized to the mixed layer depth, z_m; H was the Henry's Law constant). Finally, OCS loss by mixing was treated as a one-dimensional advection-diffusion process (mixed layer depth $-$ normalized diffusion coefficient, $K_z/z_m \times$ the observed OCS gradient with depth).

The interaction of all these terms will be embodied in the March 2000 OCS time series (Fig. 8) and was the subject of a modeling study by Najjar et al. (pers. comm.). However, some useful observations and simple calculations to quantitatively assess the relative importance of the processes in Eq. (3) can be made with these data. First, the works of Najjar et al. (1995) and von Hobe et al. (1999) suggested

that sea-air flux is a very minor loss of OCS from surface waters (averaged over the mixed layer, the maximum loss was 0.1 pmol L^{-1} h^{-1}) and can probably be ignored, leaving hydrolysis and mixing as the loss terms. The hydrolysis rate was easily calculated (i.e., during the March cruise, k_{hyd} at the surface averaged 0.07 h^{-1}) and ranged 0.2–3.1 pmol L^{-1} h^{-1} at the surface. After sunset, the OCS loss rate is due to hydrolysis plus advection-diffusion minus the dark production rate (Q, average 4.0 pmol L^{-1} h^{-1}). To crudely assess the relative contributions of hydrolysis and mixing losses, the data for OCS after sunset in Fig. 8 were fitted to Eq. (1) to derive an ''enhanced'' hydrolysis rate constant that included mixing. In this fashion, the apparent first-order hydrolysis + mixing rate constant ($k_{hyd+mix}$) was 0.62 ± 0.17 h^{-1} ($n = 7$ nights on 20–27 March), which was nearly a factor of 10 greater than the well-constrained hydrolysis rate constant. Although this calculation is rather simplistic, it clearly shows that downward mixing dominates the loss of surface water OCS and thus must be included in any model. If it is assumed that the wind speed was constant over the period (constant mixing), this hydrolysis + mixing rate constant can then be used to estimate the daytime (light) production of OCS as well. With this assumption, the rate of OCS increase in Fig. 8 (average, 5.5 ± 1.5 pmol L^{-1} h^{-1} from dawn until the observed maximum OCS; $n = 7$) is due to dark (4.0 pmol L^{-1} h^{-1}) and light production, minus hydrolysis + mixing (14.8 ± 2.2 pmol L^{-1} h^{-1} over the same period using the average of $k_{hyd+mix} \times [OCS]_t$). Keeping in mind that the mixed layer depth did vary diurnally (affecting the constant mixing assumption), this yielded a *rough* estimate of 16.4 ± 3.4 pmol L^{-1} h^{-1} for light production, which is approximately twice the average in August 1999 for the upper 5 m (9.6 pmol L^{-1} h^{-1}) measured using the optical buoys. This also reduces the dark contribution of the total daily OCS production to approximately 30%, which is very similar to calculations in other ocean regions (Flöck and Andreae 1996).

Although previous studies of OCS cycling included all the processes discussed here, few had provided direct rate measurements (e.g., dark and light production) and an integrated assessment of their effects on OCS behavior. In this respect, the Sargasso Sea results suggested that future modeling efforts should not treat dark production as a constant rate but rather as a first-order reaction (e.g., in particles or microbial biomass). Additionally, a zero-order photochemical term would probably be insufficient, because variations in DOS and CDOM (e.g., via upwelling or mixing; Fig. 4, buoy 8) strongly affect the production rate. Finally, the dark production studies in the Sargasso Sea and those from sediments in the Chesapeake Bay (Zhang et al. 1998) suggested that it is appropriate to use the term ''biogeochemistry'' when discussing the marine OCS cycle.

References

ANDREAE, M. O. 1990. Ocean-atmosphere interactions in the global biogeochemical sulfur cycle. Mar. Chem. **30:** 1–29.

———, AND R. J. FEREK. 1992. Photochemical production of carbonyl sulfide in seawater and its emission to the atmosphere. Global Biogeochem. Cycles **6:** 175–183.

ANDREWS, S. S. A., S. CARON, AND O. C. ZAFIRIOU. 2000. Photochemical oxygen consumption in marine waters: A major sink for colored dissolved organic matter? Limnol. Oceanogr. **45:** 267–277.

BENNER, R., AND M. STROM. 1993. A critical evaluation of the analytical blank associated with DOC measurements by high-temperature catalytic oxidation. Mar. Chem. **41:** 153–160.

CHARLSON, R. J., J. E. LOVELOCK, M. O. ANDREAE, AND S. G. WARREN. 1987. Oceanic phytoplankton, atmospheric sulphur, cloud albedo and climate. Nature **326:** 655–661.

COOPER, A. J. L. 1983. Biochemistry of sulfur-containing amino acids. Annu. Rev. Biochem. **52:** 187–222.

CRUTZEN, P. J. 1976. The possible importance of COS for the sulfate layer of the stratosphere. Geophys. Res. Lett. **3:** 73–76.

CUTTER, G. A., R. S. WALSH, AND C. SILVA DE ECHOLS. 1999. Production and speciation of hydrogen sulfide in surface waters of the high latitude North Atlantic Ocean. Deep-Sea Res. II **46:** 991–1010.

DONOGHUE, T., O. C. ZAFIRIOU, AND C. D. TAYLOR. 2001. Retractable surface-following sampler. Mar. Tech. Soc. **35:** 29–35.

ELLIOTT, S., E. LU, AND F. S. ROWLAND. 1989. Rates and mechanisms for the hydrolysis of carbonyl sulfide in natural water. Environ. Sci. Technol. **23:** 458–461.

FEREK, R. J., AND M. O. ANDREAE. 1984. Photochemical production of carbonyl sulfide in marine surface waters. Nature **307:** 148–150.

FLÖCK, O. R., AND M. O. ANDREAE. 1996. Photochemical and nonphotochemical formation and destruction of carbonyl sulfide and methyl mercaptan in ocean waters. Mar. Chem. **54:** 11–26.

———, ———, AND M. DRÄGER. 1997. Environmentally relevant precursors of carbonyl sulfide in aquatic systems. Mar. Chem. **59:** 71–85.

HOFMANN, D. J. 1990. Increase in the stratospheric background sulfuric acid aerosol mass in the past ten years. Science **248:** 996–1000.

HU, C., F. E. MULLER-KARGER, AND R. G. ZEPP. 2002. Absorbance, absorption coefficient, and apparent quantum yield: A comment on common ambiguity in the use of these optical concepts. Limnol. Oceanogr. **47:** 1261–1267.

KHALIL, M. A. K., AND R. A. RASMUSSEN. 1984. Global sources, lifetimes and mass balances of carbonyl sulfide (OCS) and carbon disulfide (CS_2) in the Earth's atmosphere. Atmos. Environ. **18:** 1805–1813.

LISS, P. S., AND L. MERLIVAT. 1986. Air-sea gas exchange rates: Introduction and synthesis, p. 113–127. *In* P. Buat-Ménard [ed.], The role of air-sea exchange in geochemical cycling. D. Reidel.

NAJJAR, R. G., D. J. ERICKSON III, AND S. MADRONICH. 1995. Modeling the air-sea fluxes of gases formed from the decomposition of organic matter: Carbonyl sulfide and carbon monoxide, p. 107–132. *In* R. G. Zepp and C. Sonntag [eds.], Role of nonliving organic matter in the earth's carbon cycle. Wiley.

NELSON, N. B., D. A. SIEGEL, AND A. F. MICHAELS. 1998. Seasonal dynamics of colored dissolved organic material in the Sargasso Sea. Deep-Sea Res. I **45:** 931–957.

POS, W. H., D. D. RIEMER, AND R. G. ZIKA. 1998. Carbonyl sulfide (OCS) and carbon monoxide (CO) in natural waters: Evidence of a coupled production pathway. Mar. Chem. **62:** 89–101.

PREISWERK, D., AND R. G. NAJJAR. 2000. A global, open-ocean model of carbonyl sulfide and its air-sea flux. Global Biogeochem. Cycles **14:** 585–598.

RADFORD-KNOERY, J., AND G. A. CUTTER. 1993. Determination of carbonyl sulfide and hydrogen sulfide species in natural waters using specialized collection procedures and gas chromatogra-

phy with flame photometric detection. Anal. Chem. **65:** 976–982.

———, AND ———. 1994. Biogeochemistry of hydrogen sulfide species and carbonyl sulfide in the western North Atlantic Ocean. Geochim. Cosmochim. Acta **58:** 5421–5431.

TURCO, R. P., R. C. WHITTEN, O. B. TOON, J. B. POLLACK, AND P. HAMILL. 1980. OCS, stratospheric aerosols and climate. Nature **282:** 283–286.

UHER, G., AND M. O. ANDREAE. 1997. Photochemical production of carbonyl sulfide in North Sea water: A process study. Limnol. Oceanogr. **42:** 432–442.

ULSHÖFER, V. W., O. R. FLÖCK, G. UHER, AND M. O. ANDREAE. 1996. Photochemical production and air-sea exchange of carbonyl sulfide in the eastern Mediterranean Sea. Mar. Chem. **53:** 25–39.

———, G. UHER, AND M. O. ANDREAE. 1995. Evidence for a winter sink of atmospheric carbonyl sulfide in the northeast Atlantic Ocean. Geophys. Res. Lett. **22:** 2601–2604.

VALENTINE, R. L., AND R. G. ZEPP. 1993. Formation of carbon monoxide from the photochemical degradation of terrestrial dissolved organic carbon in natural waters. Environ. Sci. Technol. **27:** 409–412.

VON HOBE, M., G. A. CUTTER, A. J. KETTLE, AND M. O. ANDREAE. 2001. Dark production: A significant source of oceanic COS. J. Geophys. Res. **106:** 31,217–31,226.

———, A. J. KETTLE, AND M. O. ANDREAE. 1999. Carbonyl sulphide in and over seawater: Summer data from the northeast Atlantic Ocean. Atmos. Environ. **33:** 3503–3514.

WEISS, P. S., S. S. ANDREWS, J. E. JOHNSON, AND O. C. ZAFIRIOU. 1995*a.* Photoproduction of carbonyl sulfide in south Pacific Ocean waters as a function of irradiation wavelength. Geophys. Res. Lett. **22:** 215–218.

———, J.E. JOHNSON, R. H. GAMMON, AND T. S. BATES. 1995*b*. Reevaluation of the open ocean source of carbonyl sulfide to the atmosphere. J. Geophys. Res. **100:** 23,083–23,092.

ZEPP, R. G., AND M. O. ANDREAE. 1994. Factors affecting the photochemical production of carbonyl sulfide in seawater. Geophys. Res. Lett. **21:** 2813–2816.

ZHANG. L. 1999. The effects of metal complexation on the oxidation of hydrogen sulfide by iodate in seawater. Ph.D. dissertation, Old Dominion Univ.

———, R. S. WALSH, AND G. A. CUTTER. 1998. Estuarine cycling of carbonyl sulfide: Production and sea-air flux. Mar. Chem. **61:** 127–142.

Received: 7 January 2003
Amended: 14 November 2003
Accepted: 20 November 2003